

Article

Comprehensive Multi-Scale Optimisation of Rum Fermentation

Tinashe W. Mangwanda ¹, Joel B. Johnson ¹, Ryan J. Batley ^{1,*}, Steve Jackson ², Tyryn McKeown ²
and Mani Naiker ^{1,3}

¹ College of Science and Sustainability, Central Queensland University, Bruce Hwy, North Rockhampton, QLD 4701, Australia; tinashe.mangwanda@ferrero.com (T.W.M.); joel.johnson@cqu.edu.au (J.B.J.); m.naiker@cqu.edu.au (M.N.)

² Bundaberg Rum Distillery, Whitred Street, Bundaberg, QLD 4670, Australia; steve.jackson@diageo.com (S.J.); tyryn.mckeown@diageo.com (T.M.)

³ Institute for Future Farming Systems, Central Queensland University, Bundaberg, QLD 4670, Australia

* Correspondence: r.j.batley@cqu.edu.au

Abstract: This study applied response surface methodology (RSM) to optimise process parameters for rum fermentation. The primary aim was to enhance ethanol productivity through refined molasses conditioning and fermentation. Polyacrylamide flocculants were evaluated for molasses clarification, identifying an optimised blend which significantly outperformed individual flocculants. Statistical analyses revealed Flopam AN 956 SH as the top performer based on settling behaviour and mud qualities. Mixture modelling exposed optimised flocculant formulations that outperformed individual flocculants, indicating synergistic interactions. A central composite design (CCD) systematically evaluated the effects of temperature, oxygenation, and nutrient supplementation on yeast growth kinetics. It determined that 5 ppm O₂, 32.19 °C, and 2.5% nutrients maximised the specific growth rate at 0.39 h⁻¹ and ethanol yield at 9.84% v/v. The models characterised interactions, revealing nutrient–oxygen synergies that stimulated metabolism. Overall, fermentation efficiency and assurance for ethanol yield were increased through comprehensive multi-scale optimisation utilising factorial designs, validated analytics, and quantitative strain characterisation.

Keywords: response surface methodology; ethanol productivity; polyacrylamide flocculants; central composite design; yeast growth kinetics; statistical optimisation



Academic Editor: Ogueri Nwaiwu

Received: 31 October 2024

Revised: 16 December 2024

Accepted: 19 December 2024

Published: 22 January 2025

Citation: Mangwanda, T.W.; Johnson, J.B.; Batley, R.J.; Jackson, S.; McKeown, T.; Naiker, M. Comprehensive Multi-Scale Optimisation of Rum Fermentation. *Beverages* **2025**, *11*, 17. <https://doi.org/10.3390/beverages11010017>

Copyright: © 2025 by the authors. Licensee MDPI, Basel, Switzerland. This article is an open access article distributed under the terms and conditions of the Creative Commons Attribution (CC BY) license (<https://creativecommons.org/licenses/by/4.0/>).

1. Introduction

Key aspects of the rum fermentation process have been previously analysed with various studies reporting the characterisation of raw materials, the definition of optimal yeast growth conditions, and the exploration of microbial community dynamics [1–3]. This study combines these significant findings to conduct targeted fermentation optimisation studies using response surface methodology (RSM). The overarching aim was to enhance ethanol productivity, yield, and process efficiency under the industrial conditions of the Bundaberg Distilling Company (BDC).

Molasses composition has a profound impact on yeast growth and fermentation kinetics in rum production. Variability in its sugar content, nitrogen levels, and potential fermentation inhibitors requires consideration to tailor and control process parameters for optimal fermentation [1,2]. The ideal temperature, pH, and oxygenation levels for yeast propagation have been previously established, and they demonstrate the influence of physicochemical parameters on fermentation performance [1,3].

The raw molasses used in rum fermentation contain a considerable amount of suspended solids when they arrive from sugar refineries which must be removed prior to

fermentation [4,5]. This clarification process reduces turbidity and yield losses, improves fermentation efficiency, and prevents fouling of downstream equipment [6]. Conventional clarification techniques involve settling or centrifugation to separate particulate matter from molasses. However, these physical methods alone are often insufficient to achieve the desired degree of clarity due to the colloidal and submicron nature of molasses solids [7]. Chemical clarification using inorganic coagulants or polymeric flocculants has thus emerged as an important pretreatment step [8,9].

Flocculants function by adsorbing to suspended solids and aggregating them into settleable flocs or flakes. This conglomerative effect accelerates gravitational separation [10]. However, a challenge exists in identifying the best performing blend of polyacrylamide flocculants from a myriad of potential combinations and proportions. This study evaluates the performance of several commercially available anionic polyacrylamide flocculants for clarifying raw cane molasses in bench-scale jar tests. Rapid screening of flocculant type and dosage provides insight towards optimising molasses pretreatment. To this end, a comprehensive yet efficient method was required to unravel the interactions between constituents that synergistically maximise solid removal. A simplex lattice design addressed this need by mapping out a limited set of mixture points that systematically covered the compositional domain for variable flocculants. Rather than testing formulations sequentially, the simplex lattice design provided insights through mathematical modelling. It deconvoluted individual component impacts from two-way interactions to reveal the true influences on clarification performance [11].

Additionally, this study also focused on further elucidating the interactive influences of oxygenation, temperature, and nutrient supplementation on yeast functionality. Continuous dissolved oxygen provisioning, maintenance of optimal thermal conditions, and supplementation of an optimised nutrient formulation emerge as top priorities for process refinement according to previous statistical analyses [1], mechanistic evidence from the literature [3,6,7], and communication with BDC personnel. Limiting the scope of research to these specific parameters streamlined experimentation whilst ensuring the applicability of results to existing manufacturing practices.

Response surface methodology is applied to quantitatively model multivariate interactions, with increased resolution afforded by a condensed three-factor design [12,13]. By more precisely characterising coordination dynamics between these select variables, tighter control ranges conducive to maximising productivity can be defined. These targeted insights are expected to enhance opportunities for knowledge-driven optimisation of the fermentation process.

This study applies a data-driven approach to leveraging the multi-factorial understanding of rum fermentation. The use of RSM is suited for navigating the complex dynamics between materials, microbes, and process conditions. The focus on industrially relevant scales and multivariate optimisation factors distinguishes this study from previous analyses of isolated parameters. The multivariate RSM approach combined with rapid hygiene monitoring provides a comprehensive optimisation of yeast fermentation and mitigation of contamination risks to improve fermentation efficiency. The findings provide actionable guidelines to enhance the consistency, efficiency, and productivity of rum fermentation. More broadly, this research will aid in optimising yeast-based processes where complex interactions between nutrients, physicochemical environment, and microbiota dictate productivity outcomes. Beyond rum, the analytical framework could guide optimisation of biofuel, pharmaceutical, food, and other biotechnology fermentations.

2. Materials and Methods

2.1. Experimental Design

This study employed a multi-faceted approach to optimise both molasses clarification and fermentation processes in rum production using *Saccharomyces cerevisiae*. Standardised laboratory protocols were developed to methodically investigate multiple factors. Commonly used industrial flocculants were evaluated for their effectiveness in clarifying raw molasses samples under controlled testing. Flocculant performance was assessed on sedimentation behaviour to identify optimal clarification aids.

Additionally, the fermentation parameters of oxygenation, temperature, and nutrient supplementation were evaluated over designated ranges using a central composite experimental design. Response surface modelling then determined the optimal factor settings to maximise ethanol yield and volumetric productivity.

2.2. Molasses Clarification Optimisation

Seven commercially available anionic polyacrylamide flocculants were evaluated: Flopam AN 923 XV, Flopam AN 934 SH, Flopam AN 934 VHM, Flopam AN 945 SH, Flopam AN 945 VHM, Flopam AN 956 SH, and Flopam AN 977 SH. These flocculants, which are synthetic high molecular weight polymers containing negatively charged functional groups, are commonly used to enhance solid–liquid separation by promoting the aggregation and settling of suspended particles. They are from the Flopam product line and were selected based on common usage in sugar clarification processes and availability from the local supplier (SNF Australia; Lara, Australia).

A Platypus (Microfloc Pty Ltd., North Rocks, Australia) 4GJT lab jar tester equipped with four 1 L glass beakers was used to simulate rapid mixing and flocculation conditions. The apparatus features adjustable paddles and timers to control stirring speeds and durations. Prior to each test, the beakers and paddles were cleaned thoroughly with detergent, rinsed with distilled water, and air dried. A 1000 mL volume of freshly collected raw molasses sample was measured into each beaker using a graduated cylinder and transferred to the jar tester platform.

The polyacrylamide flocculant solutions were prepared just before each trial by dissolving the required amount of dry powder in small volumes of distilled water. The stock solutions were gently mixed until fully dissolved. Known volumes (as per the testing dosages listed in Table 1) of the flocculant solutions were then dosed rapidly into their respective jars using micropipettes, before immediate rapid mixing at 150 rpm. This speed was selected based on preliminary trials to generate sufficient shear without disrupting the flocs. After 2 min of rapid mixing, the paddles were reduced to 60 rpm for the flocculation phase, lasting 30 min. After completion of the jar test cycle, the mixtures were allowed to settle undisturbed.

After 30 min, a distinct mud layer and clarified supernatant were clearly visible in most samples. The volume of settled mud in each beaker was then carefully recorded in millilitres (mL) using a graduated cylinder. This parameter was used as the primary response variable to evaluate flocculant performance. All procedures were carefully timed, and the stirring regimen was kept consistent between duplicate samples and across different flocculant test runs using the programmable timer controls. This ensured standardisation and reliability of the flocculation simulations.

Table 1. Experimental results for flocculant dosage optimisation. Settling time 30 min.

Flocculant	Dosage (ppm)	Supernatant Clarity (%)	Mud Layer Height (cm)	Mud Compaction
Flopam AN 923 XV	7	75 ± 0	317 ± 3	Loose, fluffy
	8	82 ± 2	283 ± 7	Moderately compact
	9	87 ± 3	249 ± 6	Moderate compaction
Flopam AN 934 SH	7	82 ± 1	298 ± 12	Loose, fluffy
	8	87 ± 2	257 ± 5	Moderately compact
	9	90 ± 3	205 ± 4	Dense, rigid
Flopam AN 934 VHM	7	72 ± 2	347 ± 3	Very loose
	8	77 ± 3	304 ± 2	Loose, fluffy
	9	82 ± 2	278 ± 3	Moderately compact
Flopam AN 945 SH	7	85 ± 3	216 ± 4	Loose, fluffy
	8	90 ± 2	176 ± 3	Moderately compact
	9	95 ± 1	143 ± 6	High compaction
Flopam AN 945 VHM	7	72 ± 1	314 ± 3	Very loose
	8	78 ± 2	283 ± 4	Loose, fluffy
	9	83 ± 1	252 ± 3	Moderately compact
Flopam AN 956 SH	7	92 ± 2	202 ± 3	Moderately compact
	8	95 ± 3	176 ± 1	High compaction
	9	98 ± 1	148 ± 2	Very high compaction
Flopam AN 977 SH	7	87 ± 2	249 ± 1	Moderately compact
	8	92 ± 1	203 ± 2	Dense, rigid
	9	96 ± 2	152 ± 1	Very high compaction

2.3. Response Surface Methodology Experimental Design

A three-factor central composite design was constructed using Stat-Ease Design Expert (version 13; Stat-Ease Inc., Minneapolis, MN, USA) software to systematically evaluate the interactive effects of oxygenation (X_1), temperature (X_2), and nutrient supplementation (X_3) on fermentation responses. X_1 (oxygenation) was set at 3 levels ranging from 0 to 10 ppm dissolved oxygen in 5 ppm increments. X_2 (temperature) was varied between 30 and 35 °C in 2.5 °C increments and X_3 (nutrient supplementation) was tested from 0 to 5% in 2.5% increments using a nutrient formulation consisting of 5 g/L $(\text{NH}_4)_2\text{SO}_4$ and 5 g/L amino acids. Each factor was investigated at axial points ($-\alpha$), factorial points ($-1, +1$), and a centre point (0) for a total of 27 experimental runs. The design structure allowed for estimation of quadratic response surfaces while accounting for curvature and the optimisation of responses. The relationship between the experimental factors and the measured fermentation responses was modeled using the polynomial regression equation

$$Y = \beta_0 + \beta_1X_1 + \beta_2X_2 + \beta_3X_3 + \beta_{11}X_1^2 + \beta_{22}X_2^2 + \beta_{33}X_3^2 + \beta_{12}X_1X_2 + \beta_{13}X_1X_3 + \beta_{23}X_2X_3$$

where Y represents the response function (sugar consumption rate or ethanol concentration), β_0 is the intercept, and $\beta_1, \beta_2, \beta_3$ are the coefficients for the linear effects of oxygenation (X_1), temperature (X_2), and nutrient supplementation (X_3), respectively. The quadratic and interaction terms ($\beta_{11}, \beta_{22}, \beta_{33}$ and $\beta_{12}, \beta_{13}, \beta_{23}$) capture the nonlinear and interactive relationships between the factors.

2.4. Fermentation Conditions

Batch fermentations were carried out in triplicate using 250 mL flasks, with each flask containing 200 mL of molasses medium supplemented with varying proportions of the optimised nutrient formulation according to the design. Flasks were submerged and secured in thermostatically controlled water baths set to predetermined temperature levels ranging from 30 to 35 °C. Sparging stones were fitted to each flask to continuously deliver

humidified airflows regulating dissolved oxygen levels from 0 to 10 ppm according to the experimental design.

2.5. Inoculation and Sampling

A standardised inoculum consisting of 10% *v/v* actively growing *Saccharomyces cerevisiae* culture (approximately 10^7 cfu mL^{-1}) was used to initiate fermentation under aseptic conditions. Samples were periodically collected after every 6 h up to 36 h to monitor fermentation progress. The responses assessed included sugar consumption rate, reflecting catabolic conversion, and final ethanol concentration after 36 h as a metric of overall metabolic efficiency under each condition tested. Each experimental run was conducted in triplicate, with the datasets averaged for statistical and modelling analyses.

2.6. Sugar and Ethanol Quantitation

A Thermo Scientific (Waltham, MA, USA) Dionex Integriion HPIC system with a Dionex AS-AP autosampler and a 150 mm Dionex CarboPac PA210-Fast-4 μm BioLC column was used for the analysis of the sugar content. Quantitation was based on an external calibration of pure glucose, sucrose, and fructose standards purchased from Sigma Aldrich (St. Louis, MO, USA). Separation was performed using a Dionex CarboPac PA-210-Fast-4 μm BioLC column, measuring 2×150 mm. The column was maintained at a temperature of 30 °C while the compartment temperature was set to 22 °C. The eluent, 1 mM KOH, was used with a flow rate of 0.2 mL/min. The instrument was equipped with a gold-on-PTFE disposable working electrode and a 62 mil electrochemical cell gasket, with an Ag/AgCl reference electrode. The sample tray temperature was set to 4 °C and the injection volume was 0.2 μL . Isocratic elution conditions were employed with a Thermo Scientific Dionex EGC 500 KOH Eluent Generator Cartridge and Dionex CR ATC-600 Continuously Regenerated Anion Trap Column as the eluent source. Ethanol concentration was measured using an Anton Paar (Graz, Austria) DMA 4500 density meter.

2.7. Statistical Analysis

One-way analysis of variance (ANOVA) was conducted to determine if significant differences existed between flocculant treatments. If ANOVA detected an overall significance ($p < 0.05$), Tukey's HSD post hoc test was used to identify specific flocculant pairs that differed in performance. A simplex lattice mixture design was constructed in Design-Expert software to comprehensively map flocculant blend ratios. The model generated responses as functions of constituent proportions. Analysis of variance on the mixture model identified significant effects. Contour plots visualised blend compositions for optimising removal of settled solids. Numerical optimisation determined the ideal flocculant mixture. This screening and mixture modelling approach statistically analysed individual flocculant efficacies as well as synergistic blend interactions to define the optimal clarification formulation.

Factorial ANOVA was conducted using Stat-Ease Design Expert software (Version 23.1.7; Stat-Ease Inc., Minneapolis, MN, USA) to evaluate the significance of individual factors and interaction terms based on *F*-values and *p*-values less than 0.05. Quadratic response surface models were fitted to estimate the main effects and correlations between variables. Numerical optimisation isolated combinations conferring maximum responses. Interaction plots visualised coordination effects between factors influencing productivity metrics. All statistical tests were conducted in R Studio (Version 4.3.2; RStudio, Boston, MA, USA).

3. Results

3.1. Flocculant Performance Evaluation

In the experimentation aimed at optimising flocculants, dosages (ppm) were systematically varied to investigate their impact on supernatant clarity, mud layer height, and mud compaction following the jar test procedure (Table 1). The values represent the mean \pm standard deviation of three replicates for each dosage level. Flopam AN 956 SH stood out as the top performer, consistently achieving the highest supernatant clarity across dosages from 7 to 9 ppm. Flopam AN 945 SH showed strong settling behaviour, achieving supernatant clarity above 95% at the 9 ppm dosage. However, its flocs were not quite as dense and compact as AN 956 SH, resulting in slightly higher residual turbidity and mud height. Flopam AN 977 SH formed stable, fast-settling flocs but yielded higher turbidity and thinner cakes than the top performers. Clarity exceeded 92% at only its highest tested dosage. Both VHM varieties (AN 945 and AN 934) demonstrated weaker flocculating abilities, failing to adequately concentrate particles into a defined settleable layer.

3.2. Optimising Flocculant Combinations: Predictive Modeling and Performance Assessment

Figure 1a displays the predicted vs. actual graph, assessing the performance of the predictive model for mud compaction. The graph contrasts the anticipated outcomes generated by the model against the actual observed values, providing a comprehensive overview of the model's reliability in predicting mud compaction under varying conditions. In Figure 1b, a contour plot depicts the intricate relationship between different flocculants and mud compaction. The contour lines on the plot represent the varying levels of mud compaction under different combinations of flocculants, offering a detailed insight into the nuanced effects of each variable.

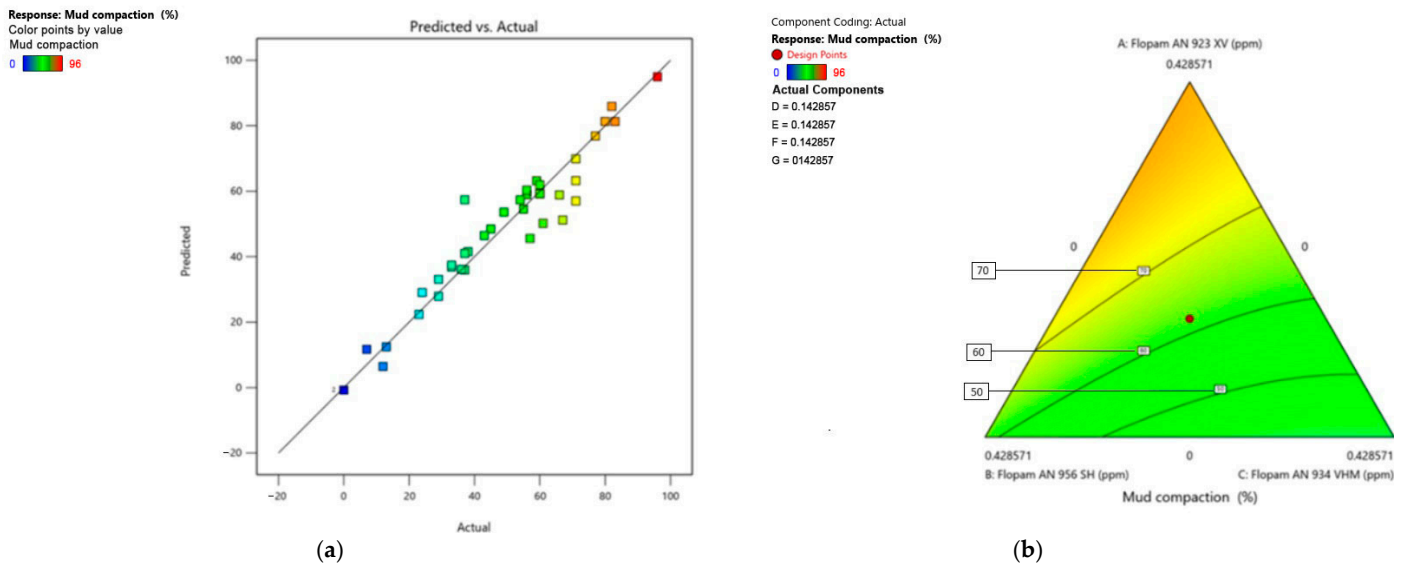


Figure 1. (a) Predicted vs. actual graph and (b) contour plots for mud compaction during molasses clarification. Comparison between predicted and actual mud compaction values obtained from response surface methodology, showing the accuracy of the model in predicting compaction behaviour. The contour plot visualises the effects of flocculant dosages on compaction, providing insight into optimal conditions for molasses clarification.

A contour plot illustrating the desirability landscape across varying levels of experimental factors is shown in Figure 2. The plot provides a visual representation of the desirability function, indicating optimal conditions for the desired mud compaction in the experimental design. The desirability scale ranges from zero, for entirely undesirable

solutions, to one, where all specified goals are fully satisfied. The plot revealed high desirability around 8.5–9 ppm dosage when Flopam AN 956 SH dominates the mixture at an 84% proportion.

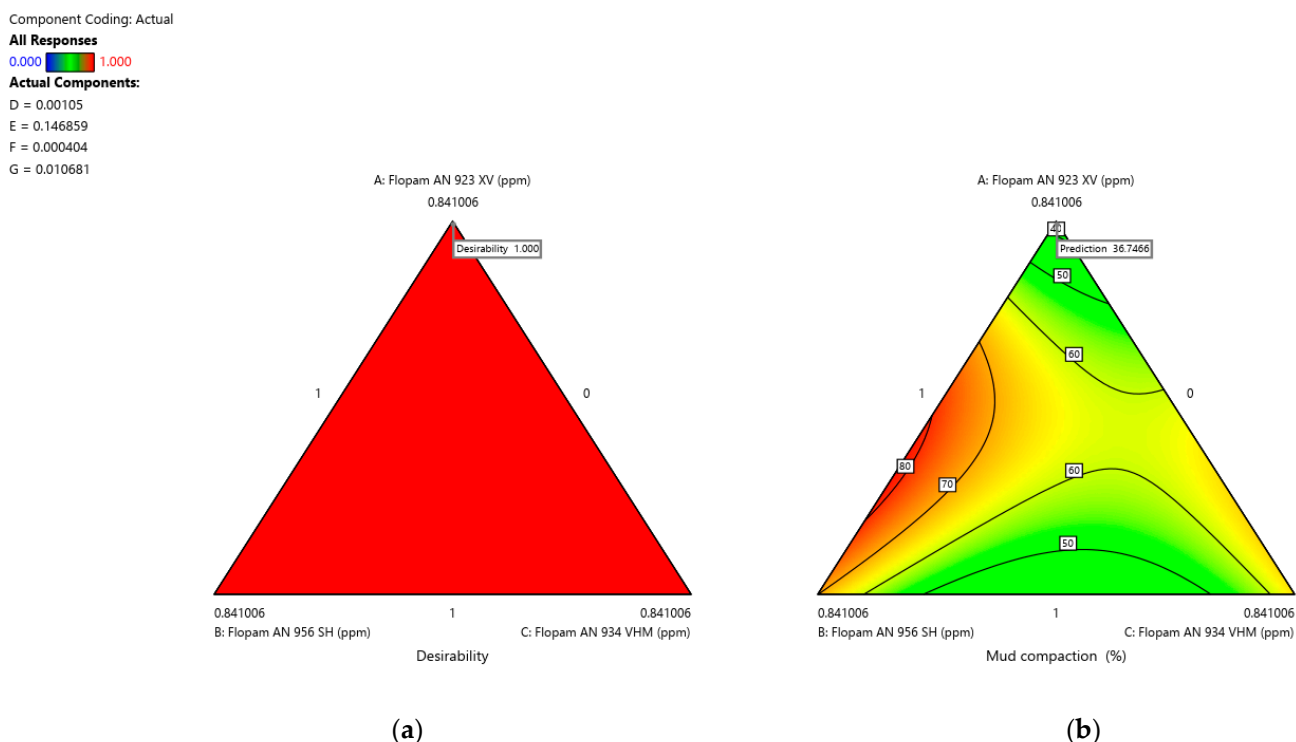


Figure 2. (a) Desirability and (b) response surface contour plots for mud compaction during molasses clarification. The plot highlights regions where optimal compaction is achieved, facilitating the selection of ideal flocculant formulations.

The interaction between flocculant dosage and mud compaction rating was further visualised using a 3D response contour plot generated in StatEase (Figure 3). The plot maps the response surface across the mixture's factor space, with dosage on the x -axis ranging from 7 to 9 ppm and relative flocculant proportions on the y -axis. The z -axis shows predicted mud compaction ratings, with higher values represented by taller peaks. Regions of elevated response are accentuated by contour lines of equal predicted response drawn at one unit intervals. As seen in Figure 3, a plateau of high compaction ratings above four forms across the dosages of 8–9 ppm for mixtures enriched in Flopam AN 956 SH. This area of optimum response agrees with the statistical models, indicating robust floc structures form within this factor combination space.

3.3. Characterising the Main Effects of Factors on Growth Kinetics

Table 2 summarises the individual effects of oxygenation, temperature, and nutrient supplementation on the maximum specific growth rate (μ_{\max}) of *Saccharomyces cerevisiae* as determined through the multi-factorial experimentation. Each factor was tested at three levels, with μ_{\max} responses reported as mean hourly rates. Varying oxygenation from 0 to 10 ppm O_2 demonstrated a significant positive influence, with 5 ppm conferring the highest μ_{\max} of 0.39 h^{-1} . Temperature exhibited a parabolic relationship as is typical, with an optimum μ_{\max} of 0.38 h^{-1} at $32.5 \text{ }^\circ\text{C}$. Linear enhancement of μ_{\max} was observed with increasing nutrient supplementation up to 5%.

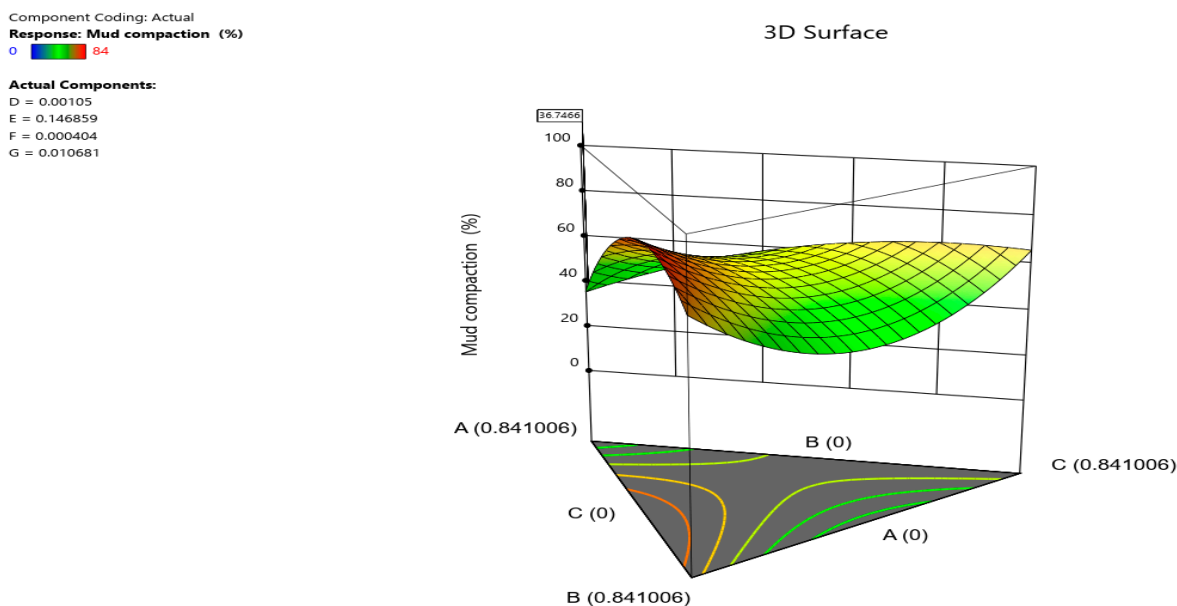


Figure 3. Three-dimensional response surface contour plot for mud compaction during molasses clarification. The plot illustrates the combined effect of these variables, pinpointing the dosage levels that maximise compaction during molasses clarification.

Table 2. Effect of process factors on maximum growth rate (μ_{max}) of *Saccharomyces cerevisiae*.

Factor	Level 1 μ_{max} (h^{-1})	Level 2 μ_{max} (h^{-1})	Level 3 μ_{max} (h^{-1})
Oxygenation (ppm)	0.35 ^a	0.39 ^b	0.31 ^c
Temperature ($^{\circ}C$)	0.37 ^a	0.38 ^b	0.32 ^a
Nutrient Supplementation (%)	0.24 ^a	0.33 ^b	0.35 ^c

Different superscript letters in the same row indicate statistically significant differences between levels based on assumed ANOVA results ($p < 0.05$).

3.4. Fermentation Multifactorial Profiler Analysis

The profiler output demonstrates the interactive effects of oxygenation (X_1) with temperature (X_2) and nutrient supplementation (X_3) on μ_{max} (Figure 4).

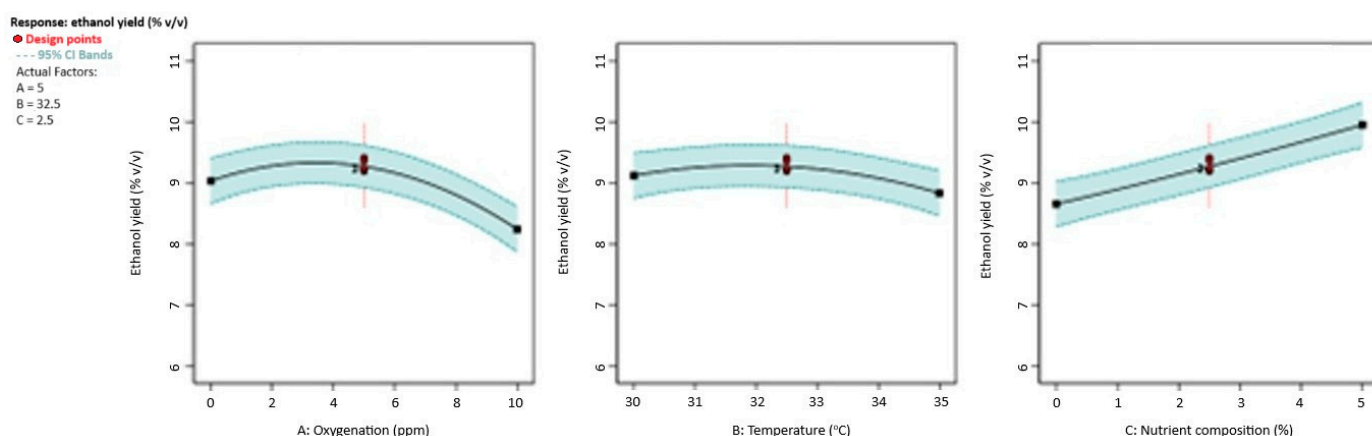


Figure 4. Profiler analysis of oxygenation, temperature, and nutrients interactions and the effect on μ_{max} . The graphical profiler analysis shows the interaction effects of oxygenation, temperature, and nutrient supplementation on the maximum specific growth rate (μ_{max}) of *Saccharomyces cerevisiae*. The profiler provides a detailed understanding of how these factors synergistically influence yeast metabolism.

3.5. Optimal Fermentation Conditions

Figure 5 illustrates an isoresponse curve mapping ethanol yield against oxygenation (horizontal axis) and temperature (vertical axis). This graphical representation reveals that at a temperature of 32.19 °C, 5 ppm oxygenation, and a 2.5% nutrient supplementation, ethanol content reaches its peak of 9.84%.

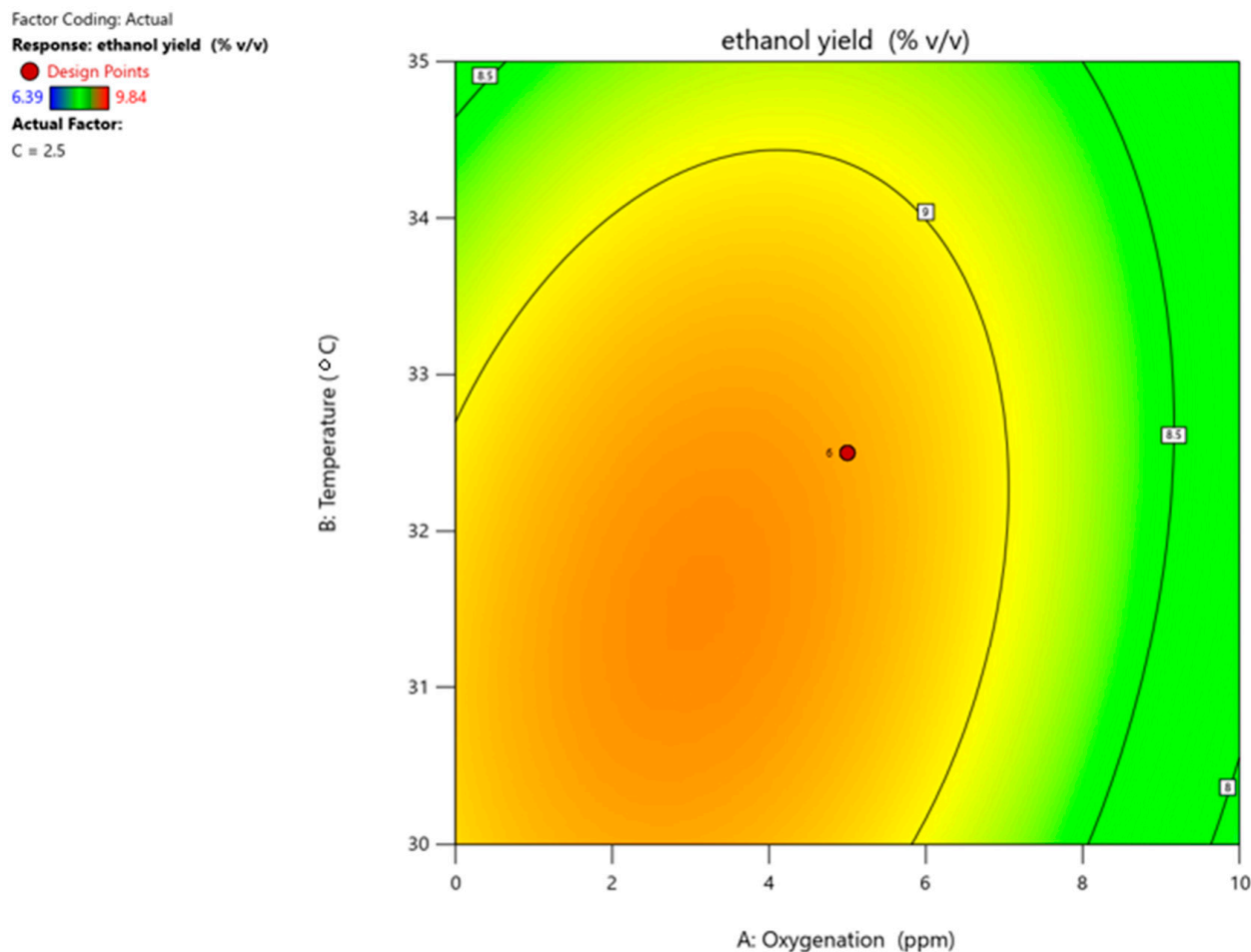


Figure 5. Fermentation isoresponse curve depicting ethanol yield under varied factorial conditions. This graph reveals the optimal fermentation conditions for maximizing ethanol yield, emphasising the combined effect of oxygenation at 5 ppm and temperature at 32.19 °C.

3.6. Response Surface Modeling

Response surface modelling generated predictive quadratic equations relating factor combinations to estimated μ_{max} responses. Figure 6 depicts this interplay, modelled as a cube plot to visualise multivariate coordination dynamics. Ridges along the X1–X2 plane indicate oxygenation and temperature jointly exert prominent positive impacts on ethanol yield progression when nutrients are in sufficient supply. Conversely, ridges along the X1–X3 axis portray a nutrient–oxygen synergy stimulating ethanol yield. Interpreting contour gradients within this 3D design space revealed conditions of maximal ethanol yield occurred at 5 ppm oxygen, 32.19 °C, and around 2.5% nutrients.

Factor Coding: Actual
 Response: ethanol yield (% v/v)
 Predicted values shown

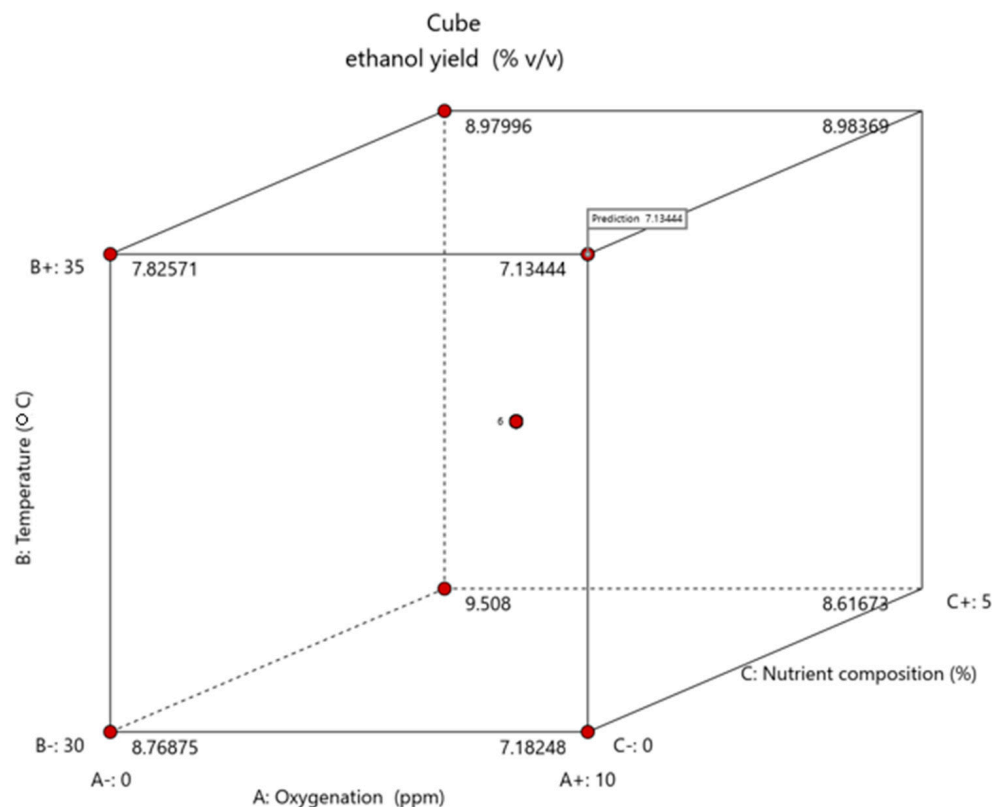


Figure 6. Cube plot from Design Expert depicting interactive influences of oxygenation, temperature, and nutrients on the predicted μ_{max} based on the quadratic response surface modelling. The quadratic response surface model depicted as a cube plot, illustrating the interactive influences of oxygenation, temperature, and nutrient supplementation on the maximum specific growth rate (μ_{max}). The plot highlights critical regions where factor interactions lead to optimal growth kinetics and ethanol yield.

4. Discussion

4.1. Optimisation of Flocculant Mixtures

In this study, response surface methodology (RSM) was employed to optimise a combination of polyacrylamide flocculants aimed at enhancing the clarification of raw molasses during rum fermentation. The utilisation of a mixture design approach was imperative to assess potential synergies among the seven commercially available flocculants that were subjected to testing. Tukey's HSD test revealed that at each dosage level, Flopam AN 956 SH produced significantly lower mud heights ($p < 0.05$) and higher compaction ratings compared to all other flocculants. For clarity, Flopam AN 956 SH and Flopam AN 945 SH achieved significantly higher percentages above 95% at the 9 ppm dosage versus other treatments.

Across the jar testing trials, Flopam AN 956 SH consistently optimised the measured response variables, demonstrating the greatest settling ability, clarity improvement, and mud dewatering effectiveness out of the evaluated flocculants. Based on its statistically superior clarification performance under the range of conditions tested, Flopam AN 956 SH can be concluded to be the top performing flocculant for clarifying raw molasses in the rum fermentation process. The chemical properties and composition of flocculants are known to strongly influence solid–liquid separation effectiveness. Flopam AN 956 SH contains high charge density and molecular weight, imparting strong bridging and sweeping activities that explain its tight, voluminous flocs.

The superior performance of Flopam AN 956 SH can be attributed to its high charge density, acrylamide content, and sulfonate functional groups, aligning well with hypothesised structure–performance relationships for molasses clarification [2,6,10]. The chemistry of Flopam AN 956 SH facilitated the formation of robust and tight floc networks, even under higher turbidity loads [14,15].

It is noteworthy that less effective individual flocculants, such as Flopam AN 934 VHM, still played a crucial role in contributing valuable data points for mapping the solution domain and aiding in statistical optimisation. A mixture design approach incorporating multiple components was necessary to fully map out the response landscape and consider potential synergistic effects between different flocculants. Even flocculants like Flopam AN 934 VHM and Flopam AN 923 XV, which showed weaker individual performances, provided data points that helped define boundaries of the solution space. Their inclusion was important for establishing the statistical models and quantifying how responses varied across the wide mixture factor range studied. Without datasets spanning the full domain, interactions and non-linear relationships may have gone undetected [12,13,16,17].

The lower performing flocculants also assisted in distinguishing true mechanistic drivers versus random variance through statistical comparison. This reinforced conclusions about advantages conferred by the intrinsic properties of Flopam AN 956 SH. The results from analysing all seven flocculant compounds will also be beneficial in the periodic re-evaluation of flocculant formulations if the characteristics of molasses changes across time. Minor adjustments may prove more effective when guided by the multidimensional insights established herein, rather than isolated re-optimisation.

The outcomes of one-way ANOVA underscored the significant main effects and interactions of both flocculant type and dosage level on all response variables. This robust statistical validation emphasises the intricate interplays between the chemistry of the flocculant and the applied conditions, as indicated by previous research [13]. Importantly, the study demonstrated that no individual flocculant, in isolation, could achieve the levels of clarification observed in the optimal mixtures identified through RSM modelling. The optimised mixtures demonstrated a notable increase in clarity and mud compaction beyond the typical outcomes achieved with single-flocculant applications. These findings suggest the presence of synergistic bridging and sweeping mechanisms in the optimised mixtures. While these results hold practical implications, it is imperative to note that further validation of the optimised formulations at larger process scales is crucial for real-world applications, representing a significant avenue for future research [18].

In that same regard, limitations in the experimental design necessitate further studies. Non-linear relationships and higher-order interactions may influence responses but were not examined due to experimental design constraints. Continuous rather than discrete dosage effects also warrant investigation. Additionally, follow-up evaluations of multi-response optimisation and scale-up behaviour could support successful industrial implementation. Nonetheless, within the ranges studied, the statistical models effectively distinguished among treatment combinations and quantified responses sensitively. This enhanced the interpretation of results beyond isolated observations. Incorporating such multivariate, knowledge-based methodologies provides a mechanism to refine clarification processes dynamically as molasses compositions vary seasonally.

4.2. Optimisation of Fermentation Kinetics

The current fermentation practices at BDC lack oxygenation and nutrient supplementation, and operate at a suboptimal temperature of 35 °C. As a result, the process yields are likely far below what is biologically attainable [6]. The findings of this study provide a knowledge base to significantly enhance the existing operation. Firstly, characterising the

individual impact of each factor establishes oxygenation and nutrient supplementation as promising leverage points to stimulate yeast metabolism and growth kinetics, given their linear positive effects on μ_{\max} . Secondly, assessing the interactive relationships demonstrates these supplemental inputs exert strong synergistic effects when combined, such as the nutrient–oxygen coordination. This highlights the benefits of adopting a systems-based optimisation approach over isolated modifications [12,13,19]. Most notably, mapping the process suggests that elevating oxygen to 5 ppm, supplementing to 5% with a mixture of ammonium sulphate and amino acids, and utilising a fermentation temperature of 32.5 °C provides maximal ethanol yield. Extrapolating from the batch experimentation results, implementing these optimised conditions in commercial fermentations could substantially increase production volume and efficiency.

Oxygenation showed a significant positive influence on μ_{\max} within the tested range (0–10 ppm), with the highest value of 0.39 h⁻¹ at 5 ppm O₂. Previous studies have reported yeast oxygen requirements around this saturation level [20]. The study noted that, for yeast to grow in anaerobic circumstances and generate lipids (sterols and unsaturated fatty acids), which are necessary for the integrity of the plasma membrane, more oxygen is typically required. Consistent with these findings, sufficient oxygenation is critical given its central metabolic role in aerobic respiration [21]. However, in the context of rum production, oxygenation introduces an additional complexity: the potential to alter the sensory profile of the product. While optimal oxygen levels enhance yeast performance and ethanol yield as shown in this study, over-oxygenation could lead to unintended flavor development due to oxidative reactions.

The temperature profile exhibited a parabolic trend, with an optimum μ_{\max} of 0.38 h⁻¹ at 32.5 °C, which aligns with yeast's known mesophilic nature [1,22,23]. Nutrient supplementation linearly enhanced μ_{\max} up to the highest tested level of 5%, reflecting cells' capacity to efficiently assimilate nitrogen and amino acids into biomass [20]. However, other authors showed that adding nitrogen raises the possibility of producing undesirable compounds, such as acetic acid [24], higher molecular weight alcohols [25], ethyl carbamate [26], and, in certain cases, hydrogen sulphide [27].

4.3. Understanding the Interactive Effect of Factors on Fermentation

Quantifying the individual factor impacts provided a baseline understanding. However, as a living system, plasticity arises from integrated regulatory networks rather than discrete components [3,13]. Accordingly, an unravelling of interactions is necessary to comprehend coordinated dynamics and thereby optimise the responses. Figure 6 provides valuable insight into the interactive influences of oxygenation and temperature on ethanol yield at a set nutrient supplementation level. The isoresponse curve mapping these two variables visually depicts their cooperative regulatory effects on fermentation performance. Certain regions of the curve indicate synergistic interactions that jointly enhance ethanol production.

Notably, the curve reveals that under the conditions evaluated, maximum ethanol yield of 9.84% occurred at an intersection temperature of 32.19 °C and oxygenation of 5 ppm. This aligns with previous understanding that moderate levels of both factors can optimise respiration to balance growth and fermentative metabolism and yields [3,13]. Interpreting the shape of the isoresponse curve and the cube plots also provides a mechanistic context. The sloping ridge indicates that temperature exerts a more influential effect on ethanol yield across its range when oxygen is limited. However, insufficient aeration constrains respiratory pathways regardless of temperature [20].

5. Conclusions

This study sought to optimise rum fermentation through a dual methodology addressing critical process parameters. Molasses clarification was first improved using a mixture design to evaluate seven polyacrylamide flocculants. Statistical analyses revealed Flopam AN 956 SH as the top performer based on settling behaviour and mud qualities. Intriguingly, mixture modelling then exposed optimised flocculant formulations which were shown to outperform individual compounds, signifying synergistic interactions between various flocculants.

Response surface methodology further characterised the influential interactive effects of temperature, oxygenation, and nutrients on critical rum fermentation responses like yeast growth, sugar usage, and ethanol yields. Numerically optimised conditions can now be validated at industrial scale in future work.

Precisely manipulating conditions and leveraging characterised strain physiology through this dual optimisation framework is anticipated to tangibly boost yields and profits through a more controlled bioprocess performance. While future designs can explore non-linear dynamics, multivariate models effectively distinguished treatments to provide actionable guidelines for knowledge-based control through combined materials and microbial and operational enhancement at BDC.

Author Contributions: Conceptualization, M.N. and T.W.M.; methodology, T.W.M. and J.B.J.; software, T.W.M.; validation, J.B.J. and M.N.; formal analysis, T.W.M.; investigation, T.W.M.; resources, M.N., T.M., S.J. and R.J.B.; data curation, T.W.M.; writing—original draft preparation, T.W.M.; writing—review and editing, T.W.M., J.B.J. and R.J.B.; visualisation, T.W.M. and J.B.J.; supervision, S.J., T.M. and M.N.; project administration, M.N.; funding acquisition, M.N. All authors have read and agreed to the published version of the manuscript.

Funding: One of the Authors, T.W.M., acknowledges funding from a Research Elevate Scholarship sponsored by CQUniversity and Bundaberg Distilling Company.

Institutional Review Board Statement: Not applicable.

Informed Consent Statement: Not applicable.

Data Availability Statement: Data are available from the authors upon request.

Acknowledgments: The authors gratefully acknowledge the technical assistance of Allison Stirrat and Karen Chadwick.

Conflicts of Interest: Two of the authors (T.M. and S.J.) are affiliated with Bundaberg Distilling Company. No other conflict of interest exists.

References

1. Basso, L.C.; de Amorim, H.V.; de Oliveira, A.J.; Lopes, M.L. Yeast selection for fuel ethanol production in Brazil. *FEMS Yeast Res.* **2008**, *8*, 1155–1163. [[CrossRef](#)]
2. Medeiros, A.B.P.; de Matos, M.E.; de Pinho Monteiro, A.; de Carvalho, J.C.; Soccol, C.R. Cachaça and rum. In *Current Developments in Biotechnology and Bioengineering: Food and Beverages Industry*; Pandey, A., Sanromán, M.Á., Du, G., Soccol, C.R., Dussap, C., Eds.; Elsevier: Amsterdam, The Netherlands, 2017; pp. 451–468.
3. Steensels, J.; Snoek, T.; Meersman, E.; Nicolino, M.P.; Voordeckers, K.; Verstrepen, K.J. Improving industrial yeast strains: Exploiting natural and artificial diversity. *FEMS Microbiol. Rev.* **2014**, *38*, 947–995. [[CrossRef](#)] [[PubMed](#)]
4. Laluce, C.; Leite, G.R.; Zavitoski, B.Z.; Zamai, T.T.; Ventura, R. Fermentation of sugarcane juice and molasses for ethanol production. In *Sugarcane-Based Biofuels and Bioproducts*; Wiley Online Library: Hoboken, NJ, USA, 2016; pp. 53–86.
5. Stolz, H.N.P. Invert Sugar from Sugar Cane Molasses: A Pilot Plant Study. Master's Thesis, University of Stellenbosch, Stellenbosch, South Africa, April 2005.
6. Mangwanda, T.; Johnson, J.B.; Mani, J.S.; Jackson, S.; Chandra, S.; McKeown, T.; White, S.; Naiker, M. Processes, challenges and optimisation of rum production from molasses—A contemporary review. *Fermentation* **2021**, *7*, 21. [[CrossRef](#)]

7. Piggot, R. Treatment and fermentation of molasses when making rum-type spirits. In *The Alcohol Textbook*, 4th ed.; Jacques, K.A., Lyons, T.P., Kelsall, D.R., Eds.; Nottingham University Press: Nottingham, UK, 2003; pp. 75–84.
8. Mahgoub, M.Y.; Gad, A.N.; El-Naggar, A.M.; Dardeer, H.M. Synthesis and Characterization of Promising Economic Biopolymer Composite as a Clarifying Agent for Sugar Industry. *Sugar Tech* **2023**, *25*, 968–981. [[CrossRef](#)]
9. Sjölin, M. Molasses Purification and Valorisation: Towards a Sustainable Production of Hydroxymethylfurfural. Ph.D. Thesis, Lund University, Lund, Sweden, 15 December 2023.
10. Green, V. The Microbial Ecology of a Rum Production Process. Ph.D. Thesis, University of New South Wales, Sydney, Australia, 2015.
11. Gorman, J.; Hinman, J. Simplex lattice designs for multicomponent systems. *Technometrics* **1962**, *4*, 463–487. [[CrossRef](#)]
12. Beigbeder, J.B.; de Medeiros Dantas, J.M.; Lavoie, J.M. Optimization of yeast, sugar and nutrient concentrations for high ethanol production rate using industrial sugar beet molasses and response surface methodology. *Fermentation* **2021**, *7*, 86. [[CrossRef](#)]
13. Pereira, L.M.S.; Milan, T.M.; Tapia-Blácido, D.R. Using Response Surface Methodology (RSM) to optimize 2G bioethanol production: A review. *Biomass Bioenergy* **2021**, *151*, 106166. [[CrossRef](#)]
14. Roselet, F.; Vandamme, D.; Roselet, M.; Muylaert, K.; Abreu, P.C. Screening of commercial natural and synthetic cationic polymers for flocculation of freshwater and marine microalgae and effects of molecular weight and charge density. *Algal Res.* **2015**, *10*, 183–188. [[CrossRef](#)]
15. Roselet, F.; Vandamme, D.; Roselet, M.; Muylaert, K.; Abreu, P.C. Effects of pH, salinity, biomass concentration, and algal organic matter on flocculant efficiency of synthetic versus natural polymers for harvesting microalgae biomass. *BioEnergy Res.* **2017**, *10*, 427–437. [[CrossRef](#)]
16. Schmidt, F. Optimization and scale up of industrial fermentation processes. *Appl. Microbiol. Biotechnol.* **2005**, *68*, 425–435. [[CrossRef](#)]
17. Singh, V.; Haque, S.; Niwas, R.; Srivastava, A.; Pasupuleti, M.; Tripathi, C. Strategies for fermentation medium optimization: An in-depth review. *Front. Microbiol.* **2017**, *7*, 2087. [[CrossRef](#)] [[PubMed](#)]
18. Zohair, F.Z.; Kabbour, M.R.; Moussaïd, S.; Ebich, F.; Bouksaim, M.; Lgaz, H.; Cho, Y.; Essamri, A. Fermentation process optimization by response surface methodology for bioethanol production from argane pulp hydrolysate using commercial and laboratory scale isolated *Saccharomyces cerevisiae* yeast. *Biomass Convers. Biorefinery* **2024**, *14*, 16891–16898. [[CrossRef](#)]
19. Slaa, J.; Gnode, M.; Else, H. Yeast and fermentation: The optimal temperature. *J. Org. Chem.* **2009**, *134*, a–c.
20. Breisha, G.Z. Production of 16% ethanol from 35% sucrose. *Biomass Bioenergy* **2010**, *34*, 1243–1249. [[CrossRef](#)]
21. Ortiz-Muñiz, B.; Carvajal-Zarrabal, O.; Torrestiana-Sanchez, B.; Aguilar-Uscanga, M.G. Kinetic study on ethanol production using *Saccharomyces cerevisiae* ITV-01 yeast isolated from sugar cane molasses. *J. Chem. Technol. Biotechnol.* **2010**, *85*, 1361–1367. [[CrossRef](#)]
22. Boulton, R.B.; Singleton, V.L.; Bisson, L.F.; Kunkee, R.E. (Eds.) Yeast and biochemistry of ethanol fermentation. In *Principles and Practices of Winemaking*; Springer: New York, NY, USA, 1999; pp. 102–192.
23. Russell, I. Understanding yeast fundamentals. In *The Alcohol Textbook*, 4th ed.; Jacques, K.A., Lyons, T.P., Kelsall, D.R., Eds.; Nottingham University Press: Nottingham, UK, 2003; pp. 531–537.
24. Bely, M.; Rinaldi, A.; Dubourdiou, D. Influence of assimilable nitrogen on volatile acidity production by *Saccharomyces cerevisiae* during high sugar fermentation. *J. Biosci. Bioeng.* **2003**, *96*, 507–512. [[CrossRef](#)] [[PubMed](#)]
25. Beltran, G.; Esteve-Zarzoso, B.; Rozès, N.; Mas, A.; Guillamón, J.M. Influence of the timing of nitrogen additions during synthetic grape must fermentations on fermentation kinetics and nitrogen consumption. *J. Agric. Food Chem.* **2005**, *53*, 996–1002. [[CrossRef](#)]
26. Ough, C.; Crowell, E.; Mooney, L. Formation of ethyl carbamate precursors during grape juice (Chardonnay) fermentation. I. Addition of amino acids, urea, and ammonia: Effects of fortification on intracellular and extracellular precursors. *Am. J. Enol. Viticult.* **1988**, *39*, 243–249. [[CrossRef](#)]
27. Wang, X.; Bohlscheid, J.; Edwards, C. Fermentative activity and production of volatile compounds by *Saccharomyces* grown in synthetic grape juice media deficient in assimilable nitrogen and/or pantothenic acid. *J. Appl. Microbiol.* **2003**, *94*, 349–359. [[CrossRef](#)] [[PubMed](#)]

Disclaimer/Publisher’s Note: The statements, opinions and data contained in all publications are solely those of the individual author(s) and contributor(s) and not of MDPI and/or the editor(s). MDPI and/or the editor(s) disclaim responsibility for any injury to people or property resulting from any ideas, methods, instructions or products referred to in the content.